IEEE Access
Multidisciplinary | Rapid Review | Open Access Journal

Received October 1, 2021, accepted October 18, 2021, date of publication October 25, 2021, date of current version November 4, 2021.

Digital Object Identifier 10.1109/ACCESS.2021.3122469

An Advanced Frequency Estimation Algorithm Based on Analytic Compensation of Effects of Dominant Harmonic in Power Systems

KYOU JUNG SON[1], GI SUNG AN[2], KYUNG DEOK NAM[2], AND TAE GYU CHANG[3], (Senior Member, IEEE)

[1]Department of Electrical Engineering, Myongji University, Yongin 17058, South Korea
[2]Maritime Sonar System, Submarine Research and Development, LIG Nex1, Seongnam 13488, South Korea
[3]Department of Electrical and Electronic Engineering, Chung-Ang University, Seoul 06911, South Korea

Corresponding author: Tae Gyu Chang (tgchang@cau.ac.kr)

This work was supported in part by the Korea Electrical Power Corporation under Grant R17XA05-02, and in part by the Chung-Ang University Research Scholarship Grants, in 2017.

ABSTRACT This paper proposes an advanced frequency estimation algorithm, where the interference effect of harmonic is effectively compensated by proposing and using a new 'harmonics interference decomposition model'. In the decomposition model, the interference effect of harmonic is represented as the sum of the two separated components, i.e., a deviation bias and an oscillatory disturbance, where the deviation bias is modeled to include only the uncoupled amplitude parameter terms and the oscillatory disturbance is modeled to exclusively include all the phase parameter coupled terms in representing a power spectral peak location. The separation and the independent compensation of the two interfering parameters significantly reduce the nonlinearity associated difficulties in deriving analytic compensation equations. Frequency estimation performance of the proposed algorithm is verified through computer simulations with diverse patterns of power system signals. The proposed algorithm's excellent estimation accuracy and rapid convergence performance are confirmed by comparing the simulation results with those of other representative algorithms.

INDEX TERMS Decomposition model, frequency estimation, harmonic interference, spectrum peak searching.

NOMENCLATURE

k	Discrete time index.
$off\_\mathfrak{I}(k)$	An imaginary part of the first off-diagonal autocorrelation value.
$off\_\Re(k)$	A real part of the first off-diagonal autocorrelation value.
$\omega_{peak}(k)$	A spectral peak location.
$R_F(k)$	Fundamental waveform parameters of $off\_\Re(k)$.
$R_{H_i}(k)$	i^{th} harmonic waveform parameters of $off\_R(k)$.
$R_O(k)$	All the remaining coupled terms of $off\_\Re(k)$.
$I_F(k)$	Fundamental waveform parameters of $off\_\mathfrak{I}(k)$.
$I_{H_i}(k)$	i^{th} harmonic waveform parameters of $off\_\mathfrak{I}(k)$.
$I_O(k)$	All the remaining coupled terms of $off\_\mathfrak{I}(k)$.
M	Highest order of harmonic.
$r(k)$	Deviation bias caused by the effect of harmonics.
$\Delta(k)$	Oscillatory disturbance caused by the effect of harmonics.
$\omega_{hc}(k)$	Harmonics compensated decomposition model of estimated frequency.
$v(k)$	Complex voltage signal.
A_1	Amplitude of the fundamental waveform.
ϕ_1	Initial phase of the fundamental waveform.
ϕ_m	Initial phase of m^{th} harmonic waveform.
A_m	Amplitude of m^{th} harmonic waveform, where $m = 2, 3, 4\ldots$.
$\omega(k)$	Fundamental angular frequency.
C	Autocorrelation matrix of $v(k)$.
$\widehat{\omega}_{bc}(k)$	Bias compensated frequency.
$\widehat{\omega}(k)$	Harmonics compensated frequency.

The associate editor coordinating the review of this manuscript and approving it for publication was Yue Zhang.

$\omega_{est}(k)$	Estimated frequency.
N	Data window length used for pre-processing.
L	Data window length used for iterative frequency update.

I. INTRODUCTION

Recently, the importance of precise and rapid frequency estimation is more emphasized as the complexity of power systems increases along with the increased use of distributed energy resources [1]–[5]. Wide variations of transient and disturbances are considered as inevitable characteristics shown in future smart grids. Highly precise and fast frequency estimation under the disturbing environment, typically interfered with the intrusion of harmonics and unbalance, becomes an important issue for rapid and reliable protection and control of power systems [3]–[8]. Since harmonics disturbance is considered as one of the major sources of performance deterioration, successful harmonic compensation is an essential task to achieve satisfactory performance level of frequency estimation.

Majority of harmonics compensation methods can be divided into two categories, i.e., analytic compensation approach [7]–[15] and stochastic modeling-based approach [5], [16]–[25]. The frequency estimation algorithms belonging to the analytic compensation approach are based on analytic derivations of waveform parameters, such as amplitudes, phases, and frequencies. With the derived waveform parameters, deviation of spectral peak location caused by harmonics interference can be directly compensated. The stochastic modeling-based approach, under the assumption of quasi-stationarity with windowed data, is based on the representation of harmonics interfering effects as stochastic model parameters. Because of well-established principle of optimization, the stochastic modeling-based method is widely adopted with diverse variations of models including adaptive filter [16], [22], [23], maximum likelihood model [4], [5], Kalman filter [18]–[20], etc..

The analytic compensation approach can be very effective if explicit and analytic estimation of the time-domain parameters are available, consequently allowing the direct application of the time-domain parameters for the compensation. However, the explicit and analytic estimation of the time-domain parameters is generally considered as a difficult task because of highly nonlinear couplings of the parameters appearing in the harmonics-interfered frequency deviation. Because of the difficulty associated with the nonlinearities, instead of direct equation solving, certain constraints and assumptions are usually adopted to limit the number of waveform parameters and/or to employ simplified signal models [13]–[15].

Based on the advantageous features of providing increased frequency resolution and statistical stability against noise and disturbance effects, the stochastic modeling-based methods show significantly improved frequency estimation performances for various harmonics included power systems [19], [24], [25]. However, in transients prevailing power systems such as in future smart grids, the trade-off characteristics between convergence rate and statistical stability of the stochastic modeling-based method becomes a significant performance limiting factor. In order to preserve high precision level with statistical stability, long enough length of data window is generally required. Longer data window, on the other hand, causes slow convergence rate, consequently resulting in the trade-off of increased estimation error during transients.

This paper proposes an advanced frequency estimation algorithm which is based on analytic compensation of effects of dominant harmonic in power systems. A harmonics decomposition model is newly proposed to mitigate the difficulty of direct equation solving required in the analytic compensation method.

In the proposed decomposition model, the effects of harmonics are separated into two components, i.e., a bias and an oscillatory disturbance. The bias is exclusively determined by the relative strength of harmonics, and the oscillatory disturbance is caused by the phase interference effect accompanied with data window sliding. Since the waveform parameters are effectively separated within the decomposition model, the bias term can be analytically compensated by deriving only the reduced number of parameters. The oscillatory component is also independently compensated resulting in high estimation precision. The issue of trade-off between convergence rate and estimation precision is effectively avoided by the application of a nonlinear filtering technique capitalizing the periodic nature of the oscillatory component.

The originality and the superiority of the proposed frequency estimation are inherited from the proposed decomposition model where all the phase parameters of a power signal are separated from the bias term, consequently enabling the independent compensation of the effect of the phase parameters.

Superior frequency estimation performance of the proposed algorithm is verified through several comparative simulations with the four representative frequency estimation algorithms, i.e., the least square smart DFT (LS-SDFT) algorithm [10], the DFT-based algorithm [9], the extended complex Kalman filters (ECKF) [19], and the demodulation algorithm [26]. It is confirmed that the proposed algorithm shows the best estimation accuracy and convergence rate among those of the frequency algorithms against various harmonics and transient reflected signals including the signals specified in the IEEE 60255-118-1: 2018 standard [27].

II. PROPOSED ANALYTIC COMPENSATION METHOD BASED ON THE DECOMPOSITION OF HARMONICS-EFFECTS

In spectral peak localization-based frequency estimation, it is generally observed, as shown in Fig. 1, that the effects of harmonics appear as distractions on the peak location having a deviation bias and a spurious oscillatory disturbance. It is shown with the analytic derivations in the following that the bias exclusively depends on the relative power ratio of the harmonics, and the oscillatory distraction is spuriously caused by

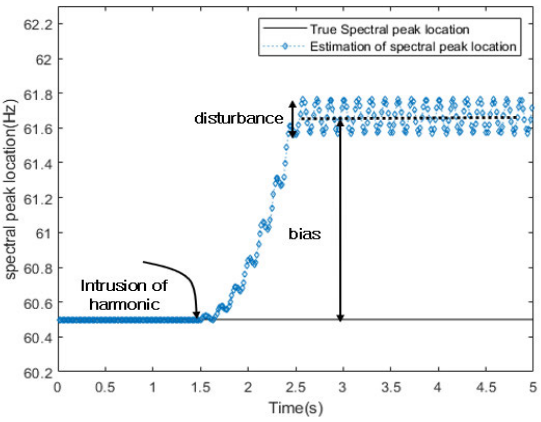

FIGURE 1. Comparison of the true frequency and spectral peak location contaminated by harmonic.

the phase interference effects associated with the time domain sliding of a processing data block. Based on this property, a 'harmonics decomposition model' is proposed, where the deviation bias is modeled to include only the uncoupled amplitude parameter terms and the oscillatory disturbance is modeled to exclusively include all the phase parameter coupled terms in representing a power spectral peak location.

When there exists no harmonic interference, the spectral peak location $\omega_{peak}\,(k)$ can be simply interpreted as the ratio of real and imaginary part of the first off-diagonal autocorrelation component, i.e., the correlation value obtained with one sample time lag, as shown in (1).

$$\omega_{peak}\,(k) = \tan^{-1}\left\{\frac{off\_\Im(k)}{off\_\Re(k)}\right\} \tag{1}$$

For harmonics included signal, the off-diagonal terms can be expressed as the sum of a fundamental terms, uncoupled harmonic terms, and the remaining coupled terms, as shown in (2).

$$\frac{off\_\Im(\mathrm{k})}{off\_\Re(\mathrm{k})} = \frac{I_F\,(k) + \sum_{i=2}^{M} I_{H_i}\,(k) + I_O\,(k)}{R_F\,(k) + \sum_{i=2}^{M} R_{H_i}\,(k) + R_O\,(k)} \tag{2}$$

The interference effects of the harmonic components can be decomposed as a deviation bias $r(k)$ and a spurious oscillatory disturbance $\Delta(k)$ parameters. By reflecting the two interfering parameters, (2) can be expressed as (3).

$$\frac{I_F\,(k) + \sum_{i=2}^{M} I_{H_i}\,(k) + I_O\,(k)}{R_F\,(k) + \sum_{i=2}^{M} R_{H_i}\,(k) + R_O\,(k)} = \frac{I_F\,(k)}{R_F\,(k)} r(k) + \Delta(k) \tag{3}$$

$$r(k) = \frac{I_F\,(k) + \sum_{i=2}^{M} I_{H_i}\,(k)}{R_F\,(k) + \sum_{i=2}^{M} R_{H_i}\,(k)} \cdot \frac{R_F\,(k)}{I_F\,(k)} \tag{4}$$

$$\begin{aligned}\Delta\,(k) = {} & \frac{I_F\,(k) + \sum_{i=2}^{M} I_{H_i}\,(k) + I_O\,(k)}{R_F\,(k) + \sum_{i=2}^{M} R_{H_i}\,(k) + R_O\,(k)} \\ & - \frac{I_F\,(k) + \sum_{i=2}^{M} I_{H_i}\,(k)}{R_F\,(k) + \sum_{i=2}^{M} R_{H_i}\,(k)}\end{aligned} \tag{5}$$

By applying (3) to (1), the proposed decomposition model is represented as (6).

$$\omega_{peak}\,(k) = \tan^{-1}\left\{\frac{I_F\,(k)}{R_F\,(k)} r(k) + \Delta(k)\right\}. \tag{6}$$

Therefore, the harmonics compensated decomposition model of the estimated frequency $\omega_{hc}(k)$ can be represented as (7).

$$\omega_{hc}(k) = \tan^{-1}\left(\frac{off\_\Im(\mathrm{k})}{off\_\Re(\mathrm{k})} * \frac{1}{r\,(k)} - \frac{\Delta(k)}{r(k)}\right) \tag{7}$$

With the harmonics compensated decomposition model of (7), the bias $r(k)$ and the oscillatory disturbance $\Delta(k)$ can be compensated separately. The closed form equation of the bias parameter $r(k)$ is analytically derived. The derivation becomes feasible because, in the decomposition model, all the phase coupled terms are separated and included in the oscillatory disturbance term $\Delta\,(k)$. The phase coupled terms, which inherently involve highly nonlinear characteristics, are considered as the major cause of the derivation difficulty. The phase parameters coupled oscillatory disturbance $\Delta(k)$ can be compensated separately by estimating oscillatory peaks and applying median filtering to the detected peaks. The disturbance compensation capitalizes the cyclic nature of the oscillatory behavior of $\Delta(k)$ to achieve accurate frequency estimation with fast convergence.

The detailed derivation process of the bias compensation equation and the oscillatory disturbance compensation are described in section III.

III. FREQUENCY ESTIMATION ALGORITHM BASED ON THE DECOMPOSITION MODEL OF DOMINANT HARMONIC INTERFERENCE

In this section, a new frequency estimation algorithm is proposed in which the effect of harmonics interference is compensated by using the decomposition model presented in section II. This section describes the frequency estimation algorithm and the derivation of the analytic equations which are designed to compensate the effect of dominant harmonic.

The target signal model $v\,(k)$, which is a complex voltage signal consisting of a fundamental and m^{th} harmonic component, is shown in (8).

$$v\,(k) = A_1(k)e^{j(\omega(k)k+\phi_1)} + A_m(k)e^{j(m\omega(k)k+\phi_m)} \tag{8}$$

The autocorrelation matrix $\boldsymbol{C}$ can be expressed as (9).

$$\begin{aligned}\boldsymbol{C} &= \begin{bmatrix} c_{11} & c_{12} \\ c_{21} & c_{22} \end{bmatrix} \\ &= \begin{bmatrix} E\left[v(k)v^*(k)\right] & E\left[v(k)v^*(k-1)\right] \\ E\left[v(k-1)v^*(k)\right] & E\left[v(k-1)v^*(k-1)\right] \end{bmatrix}\end{aligned} \tag{9}$$

The first element of the autocorrelation matrix $\boldsymbol{C}$, i.e., c_{11}, can be represented as follows.

$$\begin{aligned}c_{11} &= E\left[v(k)v^*(k)\right] \\ &= E\Big[A_1^2\,(k) + A_m^2\,(k) + A_1(k)A_m(k)\big(e^{j(\omega(k)k+\phi_1-m\omega(k)k-\phi_m)} \\ &\qquad + e^{j(m\omega(k)k+\phi_m-\omega(k)k-\phi_1)}\big)\Big]\end{aligned}$$

During the period of 'data processing window', which is set to the half cycle period, the frequency $\omega(k)$ and the amplitude $A(k)$ are considered as constant, i.e., time invariant. The effect of phase angle variation is reflected to the frequency parameter $\omega(k)$. In view of generator dynamics at faults, such assumption of quasi-stationarity is justified considering that the time constant of transient state is generally much longer than the duration of time window [28]. Then, c_{11} is obtained as follow.

$$\begin{aligned} c_{11} &= E\Big[A_1^2 + A_m^2 + A_1 A_m \big(e^{j(\omega k+\phi_1-m\omega k-\phi_m)} \\ &\qquad + e^{j(m\omega k+\phi_m-\omega k-\phi_1)}\big)\Big] \\ &= A_1^2 + A_m^2 + \beta_{11} \end{aligned} \tag{10}$$

and similarly,

$$c_{22} = A_1^2 + A_m^2 + \beta_{22} \tag{11}$$

$$c_{12} = A_1^2 e^{j\omega} + A_m^2 e^{mj\omega} + \beta_{12} \tag{12}$$

$$c_{21} = c_{12}^*. \tag{13}$$

β_{ij} contains all the fundamental and harmonic coupled terms of each element of $\boldsymbol{C}$. The detailed expression of β_{ij} is shown in Appendix A.

As shown in the following (14), the estimated peak location of the power spectrum of $v(k)$ can be obtained by applying an off-diagonal autocorrelation matrix element to (1).

$$\omega_{est\_peak}(k) = \tan^{-1}\left(\frac{\Im(c_{12})}{\Re(c_{12})}\right), \tag{14}$$

where, $\Re(\cdot)$ and $\Im(\cdot)$ denote the real and imaginary part operators, respectively. By using the proposed harmonics compensated decomposition model (7), the harmonics compensated frequency $\widehat{\omega}(k)$ can be estimated using (15).

$$\widehat{\omega}(k) = \tan^{-1}\left(\frac{\Im(c_{12})}{\Re(c_{12})} * \frac{1}{r(k)} - \frac{\Delta(k)}{r(k)}\right) \tag{15}$$

According to (4) and (5), $r(k)$ and $\Delta(k)$ can be represented as follows.

$$r(k) = \frac{A_1^2 \sin(\omega) + A_m^2 \sin(m\omega)}{A_1^2 \cos(\omega) + A_m^2 \cos(m\omega)} \cdot \frac{\cos(\omega)}{\sin(\omega)} \tag{16}$$

$$\Delta(k) = \frac{est\_\Im(c_{12})}{est\_\Re(c_{12})} - \frac{A_1^2 \sin(\omega) + A_m^2 \sin(m\omega)}{A_1^2 \cos(\omega) + A_m^2 \cos(m\omega)}, \tag{17}$$

where, $est\_\Im(c_{12})$ and $est\_\Re(c_{12})$ are the estimated values of $\Im(c_{12})$ and $\Re(c_{12})$, respectively.

From $\Re(c_{12})$ and $\Im(c_{12})$, all the fundamental and harmonic coupled terms are subtracted as shown in (18) and (19). The amplitude parameters of the fundamental and harmonic components (i.e., A_1 and A_m) can be obtained by solving (18) and (19). The analytic derivation of the amplitude parameters A_1 and A_m are shown in Appendix B. The derived analytic equations for A_1 and A_m are shown in (26) and (27), respectively.

The deviation bias $r(k)$ can be directly computed by applying the amplitude parameters to (16). The bias compensated decomposition model of the estimated frequency $\widehat{\omega}_{bc}(k)$ is represented as (20).

$$\begin{aligned} &\Re(c_{12}) - \frac{1}{2}(c_{11}+c_{22})\frac{\cos\left(\frac{(m+1)}{2}\omega\right)}{\cos\left(\frac{(m-1)}{2}\omega\right)} \\ &\quad = A_1^2\left(\cos(\omega) - \frac{\cos\left(\frac{(m+1)}{2}\omega\right)}{\cos\left(\frac{(m-1)}{2}\omega\right)}\right) \\ &\qquad + A_m^2\left(\cos(m\omega) - \frac{\cos\left(\frac{(m+1)}{2}\omega\right)}{\cos\left(\frac{(m-1)}{2}\omega\right)}\right) \end{aligned} \tag{18}$$

$$\begin{aligned} &\Im(c_{12}) - \frac{1}{2}(c_{11}+c_{22})\frac{\sin\left(\frac{(m+1)}{2}\omega\right)}{\cos\left(\frac{(m-1)}{2}\omega\right)} \\ &\quad = A_1^2\left(\sin(\omega) - \frac{\sin\left(\frac{(m+1)}{2}\omega\right)}{\cos\left(\frac{(m-1)}{2}\omega\right)}\right) \\ &\qquad + A_m^2\left(\sin(m\omega) - \frac{\sin\left(\frac{(m+1)}{2}\omega\right)}{\cos\left(\frac{(m-1)}{2}\omega\right)}\right) \end{aligned} \tag{19}$$

$$\widehat{\omega}_{bc}(k) = \tan^{-1}\left(\frac{\Im(c_{12})}{\Re(c_{12})} * \frac{1}{r(k)}\right) \tag{20}$$

The derivation of the phase parameters required in (17) is not feasible because of the involved high nonlinearities. Therefore, instead of using analytically derived equation (17), the harmonics compensated frequency of (15) is achieved by successively applying the bias compensation and the disturbance compensation using $\widehat{\omega}_{bc}(k)$.

The oscillatory disturbance $\Delta(k)$ is directly compensated by measuring the oscillatory peaks. Because of the periodic feature of the oscillatory disturbance $\Delta(k)$, the disturbance can be easily compensated by estimating the middle values between the peaks. The middle values between positive and negative peaks are estimated by applying median filtering. Median filtering, which is robust to spike-like noises, is considered as very effective to apply to the periodic natured oscillatory peaks, resulting in precise frequency estimation.

The above-described proposed frequency estimation algorithm is summarized in the flow chart shown in Fig. 2.

In the pre-processing block, a complex voltage signal is generated from a three-phase voltage signal. By using one cycle data window, the autocorrelation of the complex voltage signal is obtained, and its dominant harmonic frequency are estimated by identifying a dominant peak appearing in the DFT (discrete Fourier transform) of one cycle data.

The amplitudes of the fundamental and the harmonic frequency are estimated by applying the autocorrelation data and the previous step's estimated frequency to the analytically derived equations (26) and (27), respectively.

Harmonics compensation is achieved by successively applying the deviation bias compensation and the oscillatory disturbance compensation.

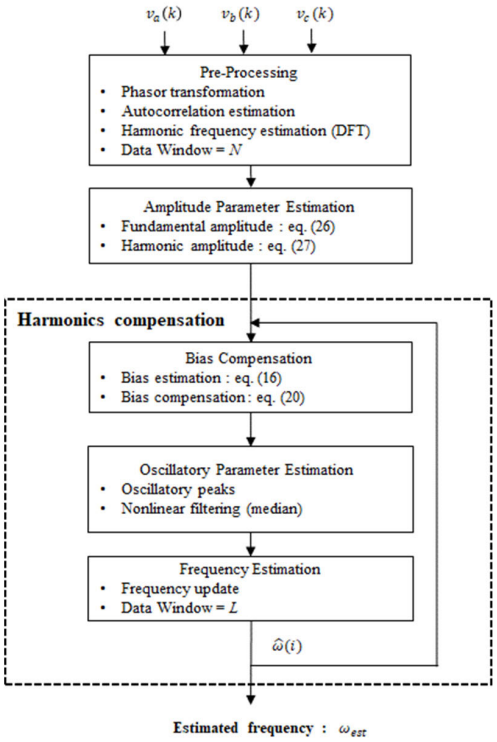

FIGURE 2. A flowchart of the frequency estimation algorithm which is based on the proposed harmonics-distraction decomposition model.

The deviation bias $r(k)$ of the proposed decomposition model, which exclusively reflects the effect of relative strength of harmonics, is estimated by directly applying the estimated values of the amplitude parameters to (16). The bias compensation is achieved by multiplying the inverse of the estimated deviation bias to the ratio of real and imaginary of the first off-diagonal autocorrelation component, i.e., $\frac{\Im(c_{12})}{\Re(c_{12})}$, as shown in (20).

The phase parameters coupled oscillatory disturbance $\Delta(k)$ is compensated separately by estimating the oscillatory peaks and applying a median filtering to the detected peaks.

For noise and oscillatory disturbance suppression, the estimated frequency $\omega_{est}\,(k)$ is iteratively updated using (21).

$$\omega_{est}\,(k) = \omega_{est}\,(k-1) + a_0\widehat{\omega}\,(k) - a_L\widehat{\omega}(k-L+1), \quad (21)$$

where, L is data window length for frequency compensation, a_0 and a_L are weighting factors.

IV. PERFORMANCE SIMULATIONS

Performances of the proposed algorithm were evaluated through computer simulations. Also, computational complexity analysis and hardware implementation of the proposed algorithm were performed to evaluate real-time application feasibility of the algorithm.

Frequency estimation performance of the proposed algorithm were compared with those of representative frequency estimation algorithms, i.e., the LS-SDFT [10], the DFT-based algorithm [9], the demodulation algorithm [26], and the ECKF algorithm [19]. For the evaluation, both 60255-118-1:2018 standard [27] referenced signals and realistic waveforms obtained from a power system simulator (EMTP-RV, CEATI Int.) were used as test signals.

In all simulation cases, the nominal frequency f_0 and sampling frequency f_s were set to 60Hz and 1920Hz, respectively. The sampling frequency is high enough, i.e., higher than twice of the highest harmonic frequency used in the simulations, to guarantee the independence from performance degradation. The length of processing data block (i.e., N) was set to 32 samples, i.e., one cycle period of the fundamental frequency, and the data window length for frequency compensation (i.e., L) was set to 16 samples, i.e., half cycle period of the fundamental frequency. For the ECKF algorithm, the dimension of the state-space model and the measurement noise covariance were set to 2 and 1.0, respectively. Also, the process noise covariance and the initial *a posteriori* estimate error covariance were set to 10^{-5} **I** and **I**, respectively, where **I** is the identity matrix. For the demodulation algorithm, a third order lowpass Butterworth filter with cutoff frequency of 25 Hz was used as a noise and harmonics reducing filter. For the LS-SDFT algorithm, the number of DFT samples and the length of the observation vector were set to 32 and the length of the vector used for a least square framework was set to 10. For the DFT-based algorithm, the length of the data window was set to P/2-10, where P is the number of sample points of a fundamental cycle.

A. SIMULATIONS WITH IEEE 60255-118-1:2018 STANDARD REFERENCED SIGNALS

The proposed algorithm was tested with the three IEEE 60255-118-1:2018 standard referenced signals (i.e., a ramp signal, an amplitude modulated signal, and a phase step change signal). The test results show that the proposed algorithm tracks the reference frequency with the smallest |FE| (absolute value of frequency error) for all the tested signals. The detailed illustrations of the simulation results are shown in the following subsections.

1) RAMP-CHANGING FREQUENCY SIGNAL WITH VARIOUS SNR (SIGNAL-TO-NOISE RATIO)

The frequency of the ramp signal varies from 58 Hz to 62 Hz with +1.0Hz/sec of ramp rate as specified in the IEEE 60255-118-1:2018 standard. A fifth harmonic component having the amplitude level as 10 % of the fundamental component was applied to the voltage signal adopting the measurement requirement of single harmonic distortion specified in the IEEE 60255-118-1:2018.

For the ramp-changing signal, the proposed algorithm precisely follows the reference frequency and the precision level is much higher than those of the other algorithms as shown in Fig. 3. The demodulation algorithm also shows good performance, but its estimation results fluctuate as the frequency varies. The DFT-based algorithm shows the largest latency since it needs relatively longer data window length of 4P to estimate frequency [9].

The summary of the maximum |FE|, which is obtained for the ramp-changing signal by varying the level of SNR

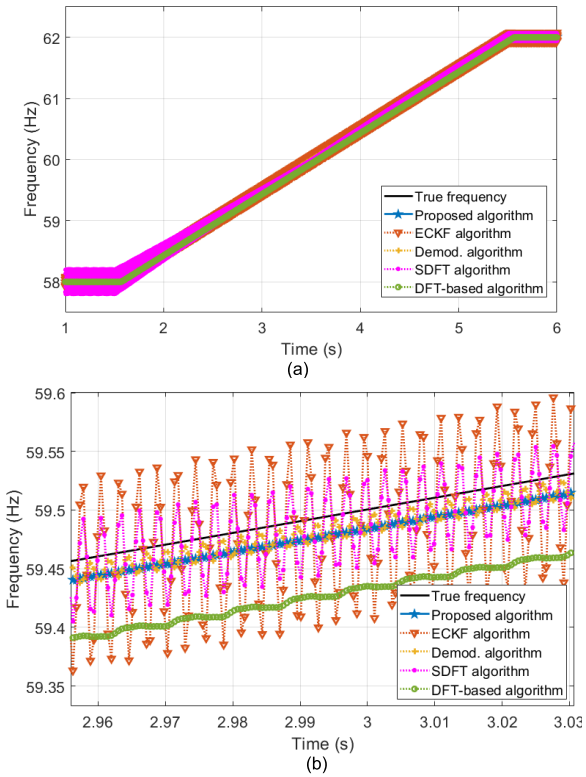

FIGURE 3. Frequency estimation results for the ramp-changing frequency signal with 10% fifth harmonic. (SNR: 80dB) (a) Results of frequency estimation, (b) Magnified view of Fig. 3(a).

TABLE 1. Maximum |FE| values for the ramp-changing signal with 10% level of fifth harmonic.

SNR / Algorithm	Max |FE| [Hz]				
	80dB	70dB	60dB	50dB	40dB
Proposed Algorithm	0.0184	0.0193	0.0218	0.0331	0.0673
ECKF Algorithm	0.0953	0.0957	0.0976	0.1069	0.1357
Demodulation Algorithm	0.0216	0.0223	0.0264	0.0412	0.0728
SDFT Algorithm	0.1869	0.1885	0.1968	0.2203	0.3348
DFT-based Algorithm	0.0724	0.0736	0.0782	0.1100	0.1787

(i.e., 40dB, 50dB, 60dB, 70dB, and 80dB), is shown in Table 1. The maximum |FE| is measured for the ramp changing transient duration. From the Table 1, it is confirmed that the proposed algorithm shows the best performance. The level of maximum |FE| of the proposed algorithm ranges from 10% to 50% compared to those of other algorithms, i.e., the ECKF, the LS-SDFT, and the DFT-based algorithm. When compared with the demodulation algorithm, which is the most comparable, the proposed algorithm shows lower level of maximum |FE| ranging from 80% to 92%.

2) AMPLITUDE MODULATED SIGNAL

An amplitude modulated signal and an added harmonic signal are also generated according to the reference specified in the 60255-118-1:2018 standard. A three-phase voltage signal was modeled by modulating its amplitude with 0.1 per unit sinusoidal variation of 1.0 Hz. The seventh harmonic component was applied to the voltage signal and its amplitude was set to 10% of the fundamental component. The system frequency was set to 59.5 Hz. The generated amplitude modulated signal is shown in Fig. 4.

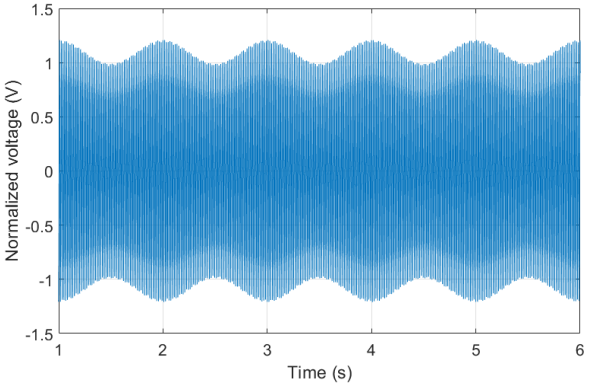

FIGURE 4. An amplitude modulated voltage signal used for performance comparison.

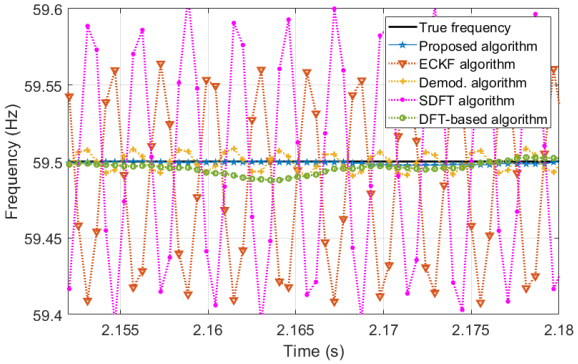

FIGURE 5. Frequency estimation results for the amplitude modulated signal with 10 % seventh harmonic (SNR: 60dB).

The frequency estimation results are illustrated in Fig. 5, where the five different patterns of frequency deviation (from the nominal frequency 59.5Hz) caused by the amplitude modulation can be well observed. From Fig. 5, it is confirmed that the proposed algorithm shows considerably higher level of robustness against the amplitude modulation compared to those of the other algorithms. The robustness results from the application of the analytically derived equations achieving precise estimation of the amplitude parameters.

Values of maximum |FE| of the frequency estimation algorithms are summarized in Table 2. It is noted that the proposed algorithm shows significantly better maximum |FE| value, i.e., 0.0069 Hz, than the maximum |FE| requirement for P-Class of the IEEE 60255-118-1 standard, i.e., 0.03 Hz, even under severer amplitude modulation test case. Comparing with the other algorithms, the level of the maximum |FE| of the proposed algorithm ranges from 6% to 51%.

TABLE 2. Maximum |FE| values for the amplitude modulated signal with 10% seventh harmonic (SNR: 60db).

Algorithm	Max |FE| [Hz]
Proposed Algorithm	0.0069
ECKF Algorithm	0.0976
Demodulation Algorithm	0.0135
SDFT Algorithm	0.1219
DFT-based Algorithm	0.0211

3) STEP CHANGE IN PHASE

A phase step change signal and an added harmonic signal are also generated according to the reference specified in the 60255-118-1:2018 standard. A three-phase voltage signal having step change in phase by $1/18\pi$ was modeled for evaluation of convergence performances of the frequency estimation algorithms. The seventh harmonic component was applied to the voltage signal and its amplitude was set to 10% of the fundamental component. The system frequency was set to 59.5 Hz.

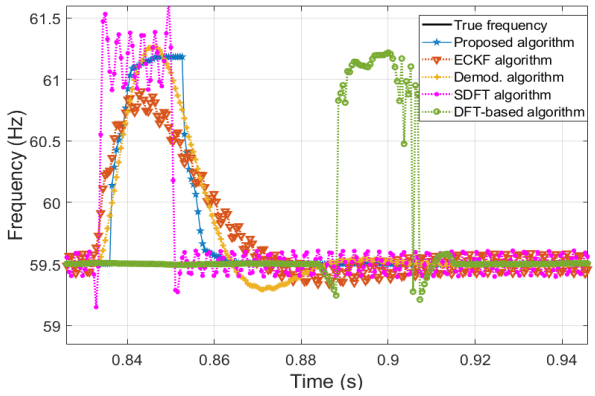

FIGURE 6. Frequency estimation results for the phase step changing signal with 10% seventh harmonic (SNR: 60dB).

Convergence patterns for the phase step change signal are shown in Fig. 6, where the convergence period of each algorithm is defined as the elapsed time from the rising moment of the step change, i.e., 0.83 second, to the moment resulting |FE| less than 0.05 Hz.

The convergence performances of each algorithm, i.e., the response time and the maximum overshoot, are summarized in Table 3. As shown in Table 3, it is confirmed that the proposed algorithm also shows the best convergence performance considering its fastest response time and significantly smaller level of maximum overshoot.

B. PERFORMANCE EVALUATION WITH REALISTIC POWER SIGNALS OBTAINED FROM A TRANSIENT SIMULATING POWER SYSTEM MODEL

In this subsection, performance of the proposed algorithm is tested with signals generated from a power system model. The signals of two cases of power system transient (i.e., load decrease by 20% and a single line-to-ground fault) were obtained from a single power plant system model which is shown in Fig. 7. For the modelling of power system, the simplified excitation system (SEXS) model, the IEEE type three-speed-Governing (IEEEG3) model, and the IEEE Stabilizing (IEEEST) model were used.

The voltage signals used for the simulations were obtained from a voltage meter (VM) module which is located at a synchronous machine (SM) side. The true frequency was obtained from rotor speed data provided by the EMTP's generator module.

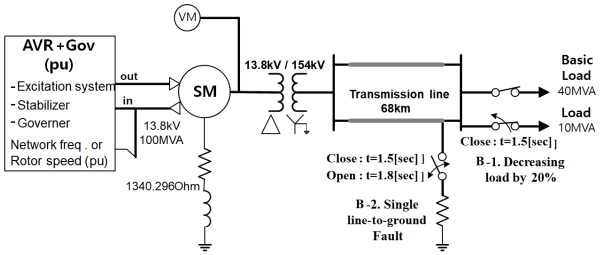

FIGURE 7. A transient signal generating power system model used for performance evaluation of the proposed algorithm.

TABLE 3. Convergence performance for the phase step changing signal with 10% seventh harmonic (SNR: 60db).

Algorithm	Convergence performance	
	Response time [sec]	Max overshoot [Hz]
Proposed Algorithm	0.0320	1.6852
ECKF Algorithm	-	1.4050
Demodulation Algorithm	0.0503	1.7607
SDFT Algorithm	-	2.1487
DFT-based Algorithm	0.0846	1.7186

1) DECREASING LOAD BY 20%

A test signal was generated by abruptly decreasing load by 20% at 1.5 second. The performance comparison of the algorithms was conducted on transient duration to avoid the effect of algorithm discontinuity at subtransient duration.

The superior performance of the proposed algorithm is well-illustrated in the frequency estimation results shown in Table 4 and Fig. 8. From Table 4, it is confirmed that the proposed algorithm shows the best estimation accuracy by showing the smallest values of maximum |FE|, |RFE|, and RMSE which ranges from 14% $\sim$ 65%, 5% $\sim$ 17%, and 18% $\sim$ 59% compared to those of the other algorithms, respectively. The subtransient duration of the test signal was excluded in calculating maximum |FE|, |RFE|, and RMSE.

2) SINGLE LINE-TO-GROUND FAULT

A single line-to-ground fault signal was generated by grounding A-phase at 1.5 second and the fault was removed by opening a switch at 1.8 second. In the same manner as the load decrease case, the performance comparison of the algorithms was conducted on transient duration to avoid the effect of algorithm discontinuity at subtransient duration.

TABLE 4. Estimation accuracy for the transient power signal (20% abrupt load decrease).

Algorithm	Estimation accuracy		
	Max |FE| [Hz]	Max |RFE| [Hz/s]	RMSE [Hz]
Proposed Algorithm	0.0093	1.2519	0.0032
ECKF Algorithm	0.0680	23.9115	0.0175
Demodulation Algorithm	0.0625	22.0600	0.0163
SDFT Algorithm	0.0142	7.8012	0.0054
DFT-based Algorithm	0.0215	7.4051	0.0145

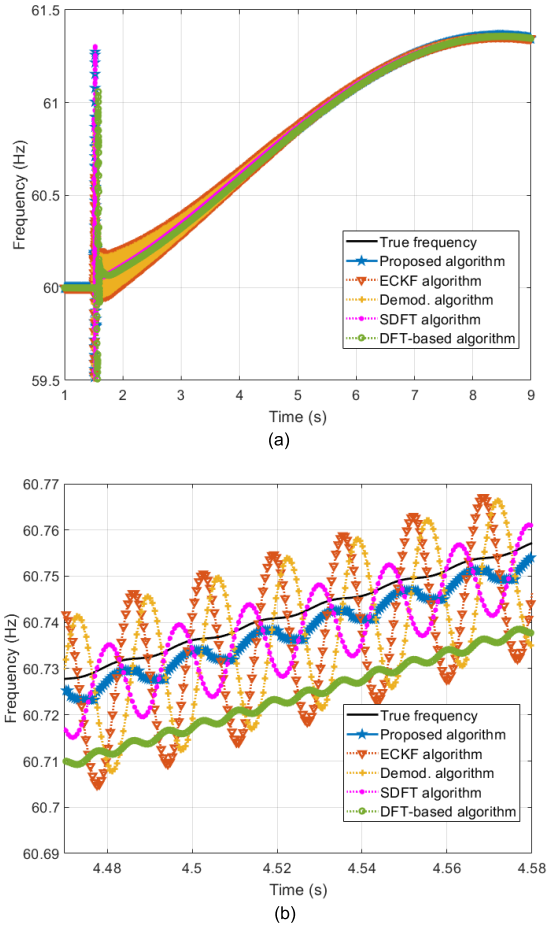

FIGURE 8. Frequency estimation results for the transient power signal obtained by simulating abruptly decreasing load by 20%. (a) Frequency estimation results, (b) Magnified view of Fig. 8(a).

Proposed algorithm's excellent convergence behavior is well observed from Fig. 9, where the proposed algorithm simultaneously shows fast convergence and significantly small fluctuations. Estimation accuracy of each algorithm is summarized in Table 5. The values of the maximum |FE|, |RFE|, and the RMSE of the proposed algorithm ranges from 8% $\sim$ 56%, 4% $\sim$ 64%, and 19% $\sim$ 100% compared to those of the other algorithms, respectively. The subtransient duration of the test signal was excluded in calculating maximum |FE|, |RFE|, and RMSE.

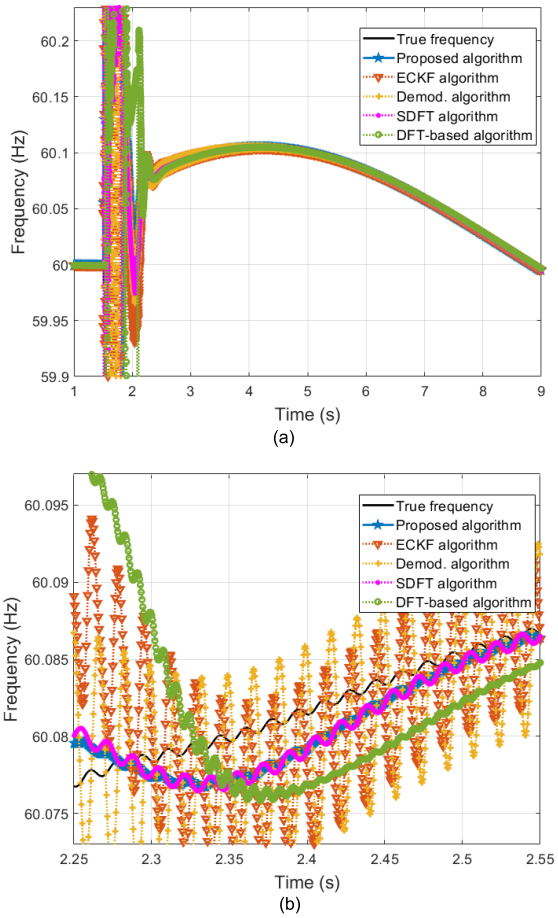

FIGURE 9. Frequency estimation results for a transient power signal obtained by simulating a single line-to-ground fault. (a) Frequency estimation results, (b) Magnified view of Fig. 9(a).

C. COMPUTATIONAL COMPLEXITY AND HARDWARE IMPLEMENTATION OF THE PROPOSED ALGORITHM

In this subsection, the computational complexity of the proposed algorithm is analyzed, and its implementation result on a MCU (microcontroller unit) system is shown.

The computational complexity of the proposed algorithm is summarized in Table 6. The computational complexity of the proposed algorithm is dominated by the process of FFT computation. The computational costs of all the other harmonic compensation processes, which are measured in terms of the real-valued multiplications, additions, and divisions, are constants and negligible when compared with that of the preprocessing block.

The proposed algorithm was implemented on a low-profile 32-bit, 150MHz MCU evaluation board to show the real-time application feasibility of the algorithm. The same algorithm parameters, which were used in the computer simulations, were applied to the implementation. The average of the processing time required for the frequency estimation is measured as about 50 microseconds. This occupies only 10% of sampling period when sampling frequency is set to typically adopted 1920Hz (32 samples per cycle). Therefore, it is

TABLE 5. Estimation accuracy for the transient power signal (single line-to-ground fault).

Algorithm	Estimation accuracy		
	Max |FE| [Hz]	Max |RFE| [Hz/s]	RMSE [Hz]
Proposed Algorithm	0.0005	0.0911	0.0003
ECKF Algorithm	0.0046	1.7760	0.0012
Demodulation Algorithm	0.0063	2.2293	0.0015
SDFT Algorithm	0.0009	0.2197	0.0003
DFT-based Algorithm	0.0023	0.1436	0.0016

TABLE 6. Computational complexity of harmonic compensation process of the proposed algorithm.

Process	Number of real value computations			Remarks
	Multiplications	Additions	Divisions	
Amplitude parameter estimation	34	28	20	-
Bias compensation	5	2	3	-
Oscillatory disturbance compensation	3	8	1	-
Pre-processing(FFT, autocorrelation computation)	O(Nlog2N)			Dominating term as N goes higher

confirmed that the proposed algorithm is feasible to implement on a low-profile embedded system for real-time application.

V. CONCLUSION

This paper proposed an advanced frequency estimation algorithm which is based on the newly introduced harmonics decomposition model. With the harmonics decomposition model, where the interference of harmonics is decomposed into the deviation bias and the oscillatory disturbance, the two interference components can be independently and separately compensated. Precise frequency estimation is achieved by applying the analytically derived harmonics compensation equation, where the nonlinearity associated difficulties in deriving the equation are significantly reduced by the separation of all the phase parameter-coupled terms into the oscillatory disturbance in the decomposition model.

The superior performance of the proposed frequency estimation algorithm is shown through the comparisons of the simulation results with those of the representative algorithms, i.e., the least square smart DFT (LS-SDFT) algorithm [10], the DFT-based algorithm [9], the extended complex Kalman filters (ECKF) [19], and the demodulation algorithm [26]. From the simulation results, it is concluded that the proposed algorithm provides precise frequency estimation by effectively compensating the interference effect of dominant harmonic.

APPENDIX A

The fundamental and harmonic coupled terms β_{11}, β_{12}, β_{21}, and β_{22} are represented as follows.

$$\beta_{11}(k) = \frac{A_1 A_m}{N} \sum_{n=k-N+1}^{k} \{2\cos((1-m)\omega n + \phi_1 - \phi_m)\} \tag{22}$$

$$\beta_{22}(k) = \frac{A_1 A_m}{N} \sum_{n=k-N+1}^{k} \{2\cos((1-m)\omega n - (1-m)\omega + \phi_1 - \phi_m)\} \tag{23}$$

$$\beta_{12}(k) = \frac{A_1 A_m}{N} \sum_{n=k-N+1}^{k} \left\{ 2\cos\left((1-m)\omega n + \phi_1 - \phi_m + \frac{(m-1)}{2}\omega\right) \cos\left(\frac{(m+1)}{2}\omega\right) + j2\cos((1-m)\omega n + \phi_1 - \phi_m + \frac{(m+1)}{2}\omega) \sin\left(\frac{(m+1)}{2}\omega\right) \right\} \tag{24}$$

$$\beta_{21}(k) = \beta_{12}^{*}(k) \tag{25}$$

N: processing data block length.

APPENDIX B

The solutions of simultaneous equations (18) and (19) (i.e., estimation of fundamental and harmonic amplitudes) can be represented as follows.

$$A_1^2 = \left\{ \frac{\left(\Re(C_{12}) - \frac{1}{2}(C_{11}+C_{22})(\cos(\omega) - cc)\right) cs_m}{cc \cdot cs_m - cs \cdot cc_m} - \frac{\left(\Im(C_{12}) - \frac{(C_{11}+C_{22})\sin(\omega) - cs}{2}\right) cc_m}{cc \cdot cs_m - cs \cdot cc_m} \right\} \tag{26}$$

$$A_m^2 = \left\{ \frac{\left(\Im(C_{12}) - \frac{(C_{11}+C_{22})(\sin(m\omega) - cc_m)}{2}\right) cc}{cc \cdot cs_m - cs \cdot cc_m} - \frac{\left(\Re(C_{12}) - \frac{(C_{11}+C_{22})(\cos(m\omega) - cc_m)}{2}\right) cs}{cc \cdot cs_m cs \cdot cc_m} \right\} \tag{27}$$

$$cc = \cos(\omega) - \frac{\cos\left(\frac{(m+1)}{2}\omega\right)}{\cos\left(\frac{(m-1)}{2}\omega\right)} \tag{28}$$

$$cc_m = \cos(m\omega) - \frac{\cos\left(\frac{(m+1)}{2}\omega\right)}{\cos\left(\frac{(m-1)}{2}\omega\right)} \tag{29}$$

$$cs = \sin(\omega) - \frac{\sin\left(\frac{(m+1)}{2}\omega\right)}{\cos\left(\frac{(m-1)}{2}\omega\right)} \tag{30}$$

$$cs_m = \sin(m\omega) - \frac{\sin\left(\frac{(m+1)}{2}\omega\right)}{\cos\left(\frac{(m-1)}{2}\omega\right)} \tag{31}$$

REFERENCES

[1] Z. Li, "A total least squares enhanced smart DFT technique for frequency estimation of unbalanced three-phase power systems," *Int. J. Electr. Power Energy Syst.*, vol. 128, Jun. 2021, Art. no. 106722.

[2] K. J. Son, G. S. An, Y. H. Kim, and T.-G. Chang, "Improved 'augmented MVDR spectrum-based frequency estimation algorithm' for unbalanced power systems," *IEEE Trans. Instrum. Meas.*, vol. 70, pp. 1–5, 2021.

[3] Y. H. Kim, K. J. Son, S.-H. Kang, and T. G. Chang, "Improved frequency estimation algorithm based on the compensation of the unbalance effect in power systems," *IEEE Trans. Instrum. Meas.*, vol. 69, no. 12, pp. 9880–9892, Dec. 2020.

[4] Y. Xia, S. Kanna, and D. P. Mandic, "Maximum likelihood parameter estimation of unbalanced three-phase power signals," *IEEE Trans. Instrum. Meas.*, vol. 67, no. 3, pp. 569–581, Mar. 2018.

[5] V. Choqueuse, A. Belouchrani, F. Auger, and M. Benbouzid, "Frequency and phasor estimations in three-phase systems: Maximum likelihood algorithms and theoretical performance," *IEEE Trans. Smart Grid*, vol. 10, no. 3, pp. 3248–3258, May 2019.

[6] H. Ahmed, M. Bierhoff, and M. Benbouzid, "Multiple nonlinear harmonic oscillator-based frequency estimation for distorted grid voltage," *IEEE Trans. Instrum. Meas.*, vol. 69, no. 6, pp. 2817–2825, Jun. 2019.

[7] A. K. Verma, R. K. Jarial, P. Roncero-Sanchez, and M. R. Ungarala, "Improved fundamental frequency estimator for three-phase application," *IEEE Trans. Ind. Electron.*, vol. 68, no. 9, pp. 8992–8998, Sep. 2020.

[8] M. S. Reza, M. M. Hossain, and M. Ciobotaru, "Teager energy operator for fast estimation of three-phase grid frequency," *IEEE Trans. Instrum. Meas.*, vol. 70, pp. 1–10, 2021.

[9] H. Xue, M. Wang, R. Yang, and Y. Zhang, "Power system frequency estimation method in the presence of harmonics," *IEEE Trans. Instrum. Meas.*, vol. 65, no. 1, pp. 56–69, Jan. 2015.

[10] Y. Xia, Y. He, K. Wang, W. Pei, Z. Blazic, and D. P. Mandic, "A complex least squares enhanced smart DFT technique for power system frequency estimation," *IEEE Trans. Power Del.*, vol. 32, no. 3, pp. 1270–1278, Jun. 2017.

[11] D. Belega and D. Petri, "Frequency estimation by two- or three-point interpolated Fourier algorithms based on cosine windows," *Signal Process.*, vol. 117, pp. 115–125, Dec. 2015.

[12] P. Romano and M. Paolone, "Enhanced interpolated-DFT for synchrophasor estimation in FPGAs: Theory, implementation, and validation of a PMU prototype," *IEEE Trans. Instrum. Meas.*, vol. 63, no. 12, pp. 2824–2836, Dec. 2014.

[13] I. Carugati, C. M. Orallo, P. G. Donato, S. Maestri, J. L. Strack, and D. Carrica, "Three-phase harmonic and sequence components measurement method based on mSDFT and variable sampling period technique," *IEEE Trans. Instrum. Meas.*, vol. 65, no. 8, pp. 1761–1772, Aug. 2016.

[14] Z. Salcic, S. Kiong Nguang, and Y. Wu, "An improved Taylor method for frequency measurement in power systems," *IEEE Trans. Instrum. Meas.*, vol. 58, no. 9, pp. 3288–3294, Sep. 2009.

[15] S. Tomar and P. Sumathi, "Amplitude and frequency estimation of exponentially decaying sinusoids," *IEEE Trans. Instrum. Meas.*, vol. 67, no. 1, pp. 229–237, Jan. 2017.

[16] M. S. Sachdev and M. M. Giray, "A least square technique for determining power system frequency," *IEEE Trans. Power App. Syst.*, vol. PAS-104, no. 2, pp. 437–444, Feb. 1985.

[17] M. M. Giray and M. S. Sachdev, "Off-nominal frequency measurements in electric power systems," *IEEE Trans. Power Del.*, vol. 4, no. 3, pp. 1573–1578, Jul. 1989.

[18] A. Routray, A. K. Pradhan, and K. P. Rao, "A novel Kalman filter for frequency estimation of distorted signals in power systems," *IEEE Trans. Instrum. Measur.*, vol. 51, no. 3, pp. 469–479, Jun. 2002.

[19] P. K. Dash, A. K. Pradhan, and G. Panda, "Frequency estimation of distorted power system signals using extended complex Kalman filter," *IEEE Trans. Power Deliv.*, vol. 14, no. 3, pp. 761–766, Jul. 1999.

[20] A. A. Girgis and T. L. D. Hwang, "Optimal estimation of voltage phasors and frequency deviation using linear and non-linear Kalman filtering: Theory and limitations," *IEEE Trans. Power App. Syst.*, vol. PAS-103, no. 10, pp. 2943–2949, Oct. 1984.

[21] V. V. Terzija, M. B. Djuric, and B. D. Kovacevic, "Voltage phasor and local system frequency estimation using Newton type algorithm," *IEEE Trans. Power Del.*, vol. 9, no. 3, pp. 1368–1374, Jul. 1994.

[22] M. Karimi-Ghartemani, A. R. Bakhshai, and M. Mojiri, "Estimation of power system frequency using adaptive notch filter," in *Proc. IEEE Instrum. Meas. Technol. Conf.*, vol. 1, Mar. 1998, pp. 143–148.

[23] A. K. Pradhan, A. Routray, and A. Basak, "Power system frequency estimation using least mean square technique," *IEEE Trans. Power Del.*, vol. 20, no. 3, pp. 1812–1816, Jul. 2005.

[24] H.-J. Jeon and T.-G. Chang, "Iterative frequency estimation based on MVDR spectrum," *IEEE Trans. Power Del.*, vol. 25, no. 2, pp. 621–630, Apr. 2010.

[25] M. Mojiri, D. Yazdani, and A. Bakhshai, "Robust adaptive frequency estimation of three-phase power systems," *IEEE Trans. Instrum. Meas.*, vol. 59, no. 7, pp. 1793–1802, Jun. 2010.

[26] M. Akke, "Frequency estimation by demodulation of two complex signals," *IEEE Trans. Power Del.*, vol. 12, no. 1, pp. 157–163, Jan. 1997.

[27] *Synchrophasors for Power Systems—Measurements*, Standard IEC/IEEE 60255-118-1, Dec. 2018.

[28] A. R. Bergen and V. Vittal, *Power Systems Analysis*, 2nd ed. Upper Saddle River, NJ, USA: Prentice-Hall, 2000.

KYOU JUNG SON received the B.S., M.S., and Ph.D. degrees in electrical engineering from Chung-Ang University, Seoul, South Korea, in 2012, 2014, and 2019, respectively.

Currently, he is a Research Professor with Myongji University, Yongin, South Korea. His research interests include area of multimedia signal processing, adaptive signal processing, and digital communication.

GI SUNG AN received the B.S. and M.S. degrees in electrical engineering from Chung-Ang University, Seoul, South Korea, in 2018 and 2020, respectively.

He is currently a Research Engineer with Nex 1 Company Ltd. His research interests include area of active noise canceling, adaptive signal processing, and frequency estimation.

KYUNG DEOK NAM received the B.S. and M.S. degrees in electrical engineering from Chung-Ang University, Seoul, South Korea, in 2017 and 2019, respectively.

He is currently a Research Engineer with Nex 1 Company Ltd. His research interests include area of adaptive signal processing, frequency estimation, and digital communication.

TAE GYU CHANG (Senior Member, IEEE) received the B.S. degree in electrical engineering from Seoul National University, Seoul, South Korea, in 1979, the M.S. degree in electrical engineering from the Korea Advanced Institute of Science and Technology, Seoul, in 1981, and the Ph.D. degree in electrical engineering from the University of Florida, Gainesville, in 1987.

Currently, he is an Emeritus Professor with Chung-Ang University.